

Transcriptional Profiling of an Attenuated *Salmonella* Typhimurium *ptsI* Mutant Strain Under Low-oxygen Conditions using Microarray Analysis

Sangyong Lim, Ahreum Han, Dongho Kim and Ho Seong Seo*

Research Division for Biotechnology, Korea Atomic Energy Research Institute, Jeongeup, Korea

Salmonella causes a wide variety of diseases ranging from mild diarrhea to severe systemic infections, such as like typhoid fever, in multiple organisms, ranging from mice to humans. A lack of *ptsI*, which encodes the first component of phosphoenolpyruvate (PEP) : carbohydrate phosphotransferase system (PTS), is known to cause *Salmonella* Typhimurium attenuation; however, the mechanisms behind this have not yet been elucidated. In this study, a DNA microarray was performed to determine why the virulence of *ptsI* mutants is attenuated under low-oxygen conditions in which the *ptsI* expression is enhanced. Of 106 down-regulated genes, the most repressed were *pdu* and *tdc* genes, which are required for propanediol utilization and threonine and serine metabolism, respectively. In addition, half the flagellar genes were down-regulated in the *ptsI* mutant strain. Because *pdu* genes are induced during infection and Tdc products and flagella-mediated motility are necessary for the invasion of *S. Typhimurium*, the invasive ability of *ptsI* mutants was examined. We found that *ptsI* mutation reduced the ability of *S. Typhimurium* to invade into host cells, suggesting that reduced expression of the *pdu*, *tdc*, and flagellar genes is involved in the attenuation of *ptsI* mutants.

Key Words: *Salmonella* Typhimurium, PTS, Flagella, Invasion

INTRODUCTION

Salmonella enterica serovar Typhimurium is an important pathogen with a broad range of hosts. *S. Typhimurium* causes self-limiting gastroenteritis, characterized by inflammatory diarrhea, in humans and cattle, but it results in a systemic disease similar to human typhoid fever in mice (1). *Salmonella* infections begin with the oral ingestion of contaminated food or water. After passing through the stomach, *Salmonella* reach and infect the small intestine by

invading through the microfold cells (M cells) in the Peyer's Patches or epithelial cells. Once across the intestinal epithelium, the *Salmonella* that cause systemic infection encounter submucosal macrophages and are localized within a membrane compartment known as the *Salmonella*-containing vacuole (SCV). Migration of infected phagocytes through the lymphatics and bloodstream disseminates *Salmonella* to the mesenteric lymph nodes and, subsequently, to the liver and spleen (2, 3).

During the course of infection, pathogenic bacteria are frequently exposed to changes in growth conditions, in-

Received: July 17, 2015/ Revised: August 5, 2015/ Accepted: August 8, 2015

*Corresponding author: Ho Seong Seo, Ph.D. Research Division for Biotechnology, Korea Atomic Energy Research Institute, 1266 Shinjung-Dong, Jeongeup 580-185, Korea.

Phone: +82-63-570-3140, Fax: +82-63-570-3149, e-mail: hoseongseo@kaeri.re.kr

**This research was supported by Nuclear R&D program of Ministry of Science, ICT & Future Planning (MSIP), Republic of Korea.

©This is an Open Access article distributed under the terms of the Creative Commons Attribution Non-Commercial License (<http://creativecommons.org/licenses/by-nc/3.0/>).

cluding pH, oxygen availability, osmotic pressure, and the supply of essential nutrients. In order to survive and efficiently replicate in host cells, pathogenic bacteria must adapt their metabolism to physical conditions and changing nutrient supplies, because the primary goal of bacteria is to gain access to nutrients rather than to cause damage to the host (4, 5). Bacterial virulence is dependent on selected general physiological responses and metabolic traits as well as on virulence genes that code for functions specifically dedicated to promoting the infection (6, 7). Indeed, several studies have shown links between carbon metabolism and pathogenic bacteria virulence (5, 8, 9).

Transcriptome analyses and isotopolog profiling experiments of *S. Typhimurium* within host cells have shown that glucose is one of the major carbon sources (10, 11). Studies have shown that the central metabolic pathway of glycolysis, a major route for glucose catabolism, is highly expressed in the SCV of macrophages and epithelial cells (10, 12) and is required for the intracellular replication of *S. Typhimurium* in both cells (13, 14). In addition, *S. Typhimurium* mutants lacking genes required for glucose uptake show reduced replication within macrophages and epithelial cells (13, 14). Taken together, these results clearly show that the ability of *S. Typhimurium* to catabolize glucose is closely linked to its virulence.

The bacterial phosphoenolpyruvate (PEP):carbohydrate phosphotransferase system (PTS) catalyzes the uptake of numerous sugars and their simultaneous phosphorylation. The PTS is composed of two cytoplasmic proteins, enzyme I (EI) and histidine protein (HPr), which are common to all PTS sugars, and membrane-bound enzyme II (EII) complex, which is specific to sugar type (15). EI, encoded by the *ptsI* gene, initiates the PTS phosphorylation chain by transferring the phosphoryl group from PEP to HPr, which is encoded by the *ptsH* gene. Finally, the phosphoryl group is transferred to sugar-specific EII complexes and, from there, to the sugar during its uptake (4). For example, glucose uptake is performed by the glucose-specific EII complex, EIIA^{Glc}, encoded by *crr*, and by EIICB^{Glc}, encoded by *ptsG* (4). Therefore, EI is required for efficient *S. Typhimurium* growth in cultured host cells (13, 14) and for a full virulent pheno-

type in mice (16).

To understand the role of EI in virulence, we surveyed the transcriptome of a *S. Typhimurium ptsI* mutant strain using DNA microarray analysis under low-oxygen conditions, because PTS mRNA is stabilized during the anaerobic growth of *Escherichia coli* (*E. coli*) cells (17). We found that *ptsI* mutation resulted in the reduced expression of *pdu*, *tdc* and flagellar genes, which are involved in *Salmonella* virulence.

MATERIALS AND METHODS

Bacterial strains and growth conditions

Salmonella Typhimurium UK1 was used as a wild type strain in this study. Isogenic *ptsI* and *mlc* mutant strains were obtained through P22HT-mediated transduction of the mutant alleles, *ptsI*::Tn10 and *mlc*::*kan*, from a *ptsI* mutant strain, JF1889, and an *mlc* mutant strain, SR1304, respectively (18). The *ptsI* mutant strain was provided by Prof. Yong Keun Park (Korea University, Korea). *S. Typhimurium* was routinely cultivated at 37°C in Luria-Bertani (LB) medium (Difco, Franklin Lakes, NJ) or on LB agar (Difco). A stationary-phase culture that had been grown overnight with shaking was used as the stock culture. The stock culture was inoculated into fresh LB broth at 1:100 dilution and then grown statically to mid-log phase (low-oxygen conditions). Tetracycline and kanamycin (Sigma-Aldrich, St. Louis, MO) were used when necessary at 15 and 50 µg/ml, respectively.

Microarray analysis

Probe preparation

Total bacterial RNA was isolated from cells grown statically to mid-log phase (O.D₆₀₀ = ~0.35) using an SV total RNA isolation kit (Promega, Madison, WI) according to the manufacturer's instructions. A total of 75 µg of RNA with 3 µg of random hexamer dissolved in 29.5 µl of nuclease free-water was denatured at 65°C for 10 min and then placed on ice. After the addition of 6 µl of 0.1 M DTT, 12 µl of first-strand buffer (5x), 1.5 µl of dNTP mix (25 mM dATP, 25 mM dGTP, 25 mM dCTP, 10 mM dTTP), 4 µl of reverse transcriptase (Superscript II[®], Invitrogen, Grand

Island, NY), 2 μ l of RNasin (Promega), and 4 μ l of either Cy3- or Cy5-conjugated dUTP (Amersham Biosciences, Buckinghamshire, UK), the labeling mixture, totaling 60 μ l, was incubated at 42 °C for 2 h and supplemented with 2 μ l of Superscript II at the end of the first hour. Each probe was denatured with 10 μ l of 1 M NaOH and neutralized with 10 μ l of 1 M HCl, followed by purification with a PCR purification kit (Qiagen, Venlo, Netherlands) and concentration with a speed vacuum drier. Each probe, separately labeled with Cy3 or Cy5, was resuspended in 20 μ l of distilled water.

Hybridization and data acquisition

Details concerning the construction and characteristics of the *Salmonella* microarray used in this study have been described elsewhere (19). Briefly, 97.5% of all 4,498 genetic elements annotated in *S. Typhimurium* LT2 are represented in triplicate on the array, as are 104 of the 109 annotated genetic elements of the virulence plasmid pSLT. Immediately before use, equal volumes of labeled probes (each 20 μ l) from the wild-type and the *ptsI* mutant strain were mixed with 40 μ l of 2x hybridization solution consisting of 50% formamide, 10x SSC, and 0.2% SDS and denatured by boiling for 5 min. Probes were simultaneously hybridized to a chip overnight at 42 °C in a hybridization chamber (Corning, Corning, NY) submerged in water. For hybridization protocols, see http://www.corning.com/Lifesciences/technical_information/techDocs/gaps_ii_manual_protocol_5_02_cls_gaps_005.pdf. Scans were performed with a Scan Array 5000 laser scanner using ScanArray 2.1 software (Packard BioChip Technologies, Billerica, MA).

Data analysis

Signal intensity was quantified using QuantArray 3.0 software (Packard BioChip Technologies). Spots were analyzed by adaptive quantification, an algorithm in the QuantArray software that compares the spot and median background intensities for each spot based on user-defined mask parameters for spot size and background diameter. The signal thresholds for spot and background are dynamic for every spot, which facilitates computational compensation for irregular spot shapes (<http://las.perkinelmer.com/content/Manuals/Quantarraymanual.pdf>). The local background in-

tensity was subsequently subtracted from the recorded spot intensities. Print-tip loess normalization within one array and scale normalization between arrays was applied for nine data points obtained from three biological replicates with swapping dyes using statistical programming environment R (<http://www.bioconductor.org>). The significance of differential expression, relative to control, was assessed using a paired *t*-test and a Bayesian analysis because Bayesian estimates of the within treatment variation tend to reduce the rate of false positives (20). The threshold for a significant change in gene expression was set at a *p*-value less than 0.001. Of the genes passing this threshold, only those with a Bayesian confidence value (B-value) above zero were regarded as being affected by the *ptsI* mutation. B-values were computed from the Cyber-T (cybert.microarray.ics.uci.edu).

Quantitative real-time PCR (qRT-PCR) analysis

Total RNA was prepared from bacterial cultures with the RNeasy mini kit (Qiagen) according to the manufacturer's instructions. qRT-PCR analysis was performed as described previously (19). The mRNA expression levels of the target gene were normalized to the 16S rRNA (*rrsH*) expression level. The sequences of the primers used are presented in Table 1.

Motility assay

Bacteria were grown to stationary phase, and a 10 μ l aliquot of each cell culture was spotted onto semi-solid (0.35%) LB agar plates that were then incubated at 37 °C. The diameter of the growth halo was measured after 7 h and 14 h on three different LB agar plates for each strain.

Invasion assay (gentamicin protection assay)

HEp-2 (ATCC CCL-23) cells, a line established from a human epidermoid carcinoma, were maintained in RPMI 1640 containing 10% FBS, penicillin (100 U/ml), and streptomycin (100 g/ml) at 37 °C under 5% CO₂. RAW 264.7 cells (ATCC, Manassas, VA), a murine macrophage-like cell line, were maintained in Dulbecco's modified Eagle medium (DMEM; Life Technologies, Carlsberg, CA) supple-

Table 1. List of primers used in qRT-PCR

Gene	Forward (5' → 3')	Reverse (5' → 3')
<i>ptsG</i>	GTCGGTTCCGCTAACTTCAG	CCCGTATCAGCAAGGTGTTT
<i>ulaC</i>	TGCTGGGAACCTGGTTATCT	TTTGGTGCTGCTGAACAATC
<i>flhD</i>	CAACGAAGAGATGGCAAACA	GACGCGTTGAAAGCATGATA
<i>fliA</i>	CCGCTGAAGGTGTAATGGAT	CCGCATTTAATAACCCGATG
<i>fliZ</i>	AAACATTTCCCACGATCTGC	CGGTAAAGGGGGATTCTGT
<i>flgM</i>	CCTTTGAAACCCGTTAGCAC	GCCGTTTTTAATGCTTCGAC
<i>fliC</i>	AACGACGGTATCTCCATTGC	TACACGGTCGATTTCGTTCA
<i>rrsH</i>	CGGGGAGGAAGGTGTTGTG	CAGCCCGGGGATTTCACATC

mented with 10% fetal bovine serum (FBS; Lonza, Basel, Switzerland), penicillin (100 U/ml; Life Technologies), and streptomycin (100 g/ml; Life Technologies) at 37°C under 5% CO₂. Cell cultures were replaced after passage number 20. For the invasion assay, 2×10^5 RAW264.7 cells were seeded into each well of a 24-well plate and incubated overnight. Bacteria [2×10^6 colony-forming units (CFU)] washed with PBS and suspended in pre-warmed DMEM were then added to the cell monolayer at an infection multiplicity of about 1:10. Following a 1 h incubation at 37°C, macrophage were washed three times with pre-warmed PBS to remove extracellular bacteria and incubated for 2 h in pre-warmed DMEM (Life Technologies) supplemented with 100 µg/ml gentamicin (Gm; Life Technologies) to kill the extracellular adherent bacteria. The monolayer was subsequently washed three times with PBS (Lonza), lysed in 1% Triton X-100 (Sigma-Aldrich) for 10 min, and diluted with PBS. Dilutions of the suspension were plated on LB agar medium to determine CFU. The experimental conditions for measuring the invasion abilities of *S. Typhimurium* strains in HEP-2 were the same as those described above for the infection of RAW 264.7, except RPMI 1640 (Life Technologies) was used as the medium.

RESULTS

Global transcriptional profiling of a *ptsI* mutant

To determine which *Salmonella* genes were altered by

ptsI mutation, a DNA microarray analysis was performed. Total RNA was extracted from the cultures grown under low-oxygen conditions and was used to make cDNA that was labeled and hybridized to a microarray (see Materials and Methods). Statistical analysis showed that 53 genes were induced and 106 genes were reduced in the *ptsI* mutant relative to the wild type (Tables 2 and 3). An overview of the genes whose expressions were altered by *ptsI* mutation was obtained by defining the functional categories of genes based on Clusters of Orthologous Groups (COG) analysis (Fig. 1).

Up-regulation of genes associated with PTS

The microarray data showed that the expression of genes associated with carbohydrate metabolism was increased in *ptsI* mutants (Fig. 1). Analysis of genes whose expression increased more than four-fold also showed that some PTS-associated genes were highly expressed in *ptsI* mutants (Table 4): the *ulaABC* genes, which encode components of L-ascorbate PTS transporter, and the *mtlA* and *ptsG* genes, which encode the mannitol- and glucose-specific PTS permeases, respectively. In addition, the expression of *manY*, which encodes the mannose-specific EIIC, was increased approximately three-fold in *ptsI* mutants (Table 2). Mlc is a global transcriptional repressor of several glucose-related genes, including *ptsG* and the *manXYZ* operon. When glucose is present, PtsG (EIICB^{Glc}) is dephosphorylated and binds the transcription factor Mlc, thus relieving repression

Table 2. The genes induced by *ptsI* mutation

Locustag	Gene name	Ratio (ptsI/wt)	<i>p</i> -value	B-value	Description
STM2342	ulaA	53.09	1.4E-09	12.49	Ascorbate-specific PTS system EIIC
STM2341		46.19	8.4E-10	12.92	Putative transketolase
STM2340		33.89	3.0E-09	11.80	Putative transketolase
STM2344	ulaC	26.92	6.7E-10	13.13	Putative PTS system EIIA component
STM3685	mtlA	26.79	5.3E-09	11.27	PTS family, mannitol-specific enzyme IIABC components
STM2343	ulaB	21.69	6.8E-11	14.99	PTS system EIIB component
STM3686	mtlD	15.80	1.7E-10	14.28	Mannitol-1-phosphate dehydrogenase
STM2339	yfcC	12.87	4.9E-09	11.34	Putative integral membrane protein
STM3687	mtlR	7.76	2.0E-09	12.14	Repressor for mtl
STM2458	eutB	6.00	1.7E-05	3.24	Ethanolamine ammonia-lyase, heavy chain
STM2462	eutJ	5.38	7.9E-05	1.63	Paral putative heatshock protein (Hsp70)
STM1203	ptsG	5.03	3.5E-07	7.20	Sugar Specific PTS family, glucose-specific IIBC component
STM2456	eutL	4.55	2.2E-04	0.58	Putative carboxysome structural protein, ethanolamine utilization
STM2459	eutA	4.24	1.2E-06	5.96	CPPZ-55 prophage; chaperonin in ethanolamine utilization
STM4007	glnA	3.99	3.6E-07	7.19	Glutamine synthetase
STM0759	ybgS	3.98	1.6E-06	5.68	Putative homeobox protein
STM2457	eutC	3.93	1.4E-05	3.44	Ethanolamine ammonia-lyase, light chain
STM1493		3.40	4.3E-05	2.26	Putative periplasmic component, ABC transport system
STM1831	manY	3.07	2.1E-05	3.01	Sugar Specific PTS family, mannose-specific enzyme IIC
STM2455	eutK	3.06	1.7E-04	0.84	Putative carboxysome structural protein, ethanolamine utilization
STM2460	eutH	2.79	3.1E-05	2.61	Putative transport protein, ethanolamine utilization
STM1491		2.71	2.4E-05	2.85	ABC-type proline/glycine betaine transport systems, ATPase component
STM1844	hspX	2.69	1.7E-04	0.85	Heat shock protein, integral membrane protein
STM1070	ompA	2.68	1.0E-05	3.77	Putative hydrogenase, membrane component
STM3384	yhdG	2.64	3.3E-05	2.54	Putative TIM-barrel enzyme, possibly dehydrogenase
STM1212	ycfJ	2.54	2.5E-04	0.42	Putative outer membrane lipoprotein
STM1929	otsB	2.52	5.2E-05	2.07	Trehalose-6-phosphate phosphatase, biosynthetic
STM0833	ompX	2.48	2.0E-06	5.43	Outer membrane protease, receptor for phage OX2
STM0852	yliG	2.47	7.7E-06	4.04	Putative Fe-S oxidoreductases family 1
STM1731		2.43	1.1E-04	1.25	Putative catalase
STM0853	yliH	2.40	1.4E-04	1.02	Putative cytoplasmic protein
STM0838	ybiT	2.39	3.3E-04	0.14	Putative ATPase component of ABC transporter with duplicated ATPase domain
STM0870		2.36	6.4E-06	4.23	Putative transport protein
STM2781	virK	2.36	1.9E-04	0.74	Virulence gene; homologous sequence to virK in <i>Shigella</i>
STM1890	yebA	2.35	2.5E-04	0.45	Putative peptidase
STM0834	ybiP	2.32	5.4E-06	4.41	Putative Integral membrane protein

Table 2. Continued

Locustag	Gene name	Ratio (ptsI/wt)	<i>p</i> -value	B-value	Description
STM1242	envE	2.30	3.5E-05	2.48	Putative envelope protein
STM1730	yciE	2.21	4.7E-05	2.18	Putative cytoplasmic protein
STM2795	ygaU	2.16	2.7E-04	0.36	Putative LysM domain
STM2780	pipB2	2.14	9.3E-06	3.85	Homologue of pipB, putative pentapeptide repeats (8 copies)
STM0478	aefA	2.14	1.1E-05	3.66	Putative small-conductance mechanosensitive channel
STM4231	lamB	2.09	2.0E-04	0.64	Phage lambda receptor protein; maltose high-affinity receptor
STM1849		2.07	2.2E-04	0.54	Putative inner membrane protein
STM1285	yeaG	2.07	1.9E-04	0.69	putative Ser protein kinase
STM1234	trmU	2.06	2.0E-05	3.08	tRNA (5-methylaminomethyl-2-thiouridylate)-methyltransferase
STM2116	wzc	2.06	3.4E-04	0.12	Putative tyrosine-protein kinase in colanic acid export
STM1827		2.05	1.3E-04	1.14	Putative diguanylate cyclase/phosphodiesterase
STM2924	rpoS	2.05	3.1E-05	2.60	Sigma S (sigma 38) factor of RNA polymerase, major sigmafactor during stationary phase
STM3506	feoB	2.02	6.4E-05	1.84	FeoB family, ferrous iron transport protein B
STM1843		2.02	6.2E-05	1.88	Putative transport protein
STM4240	yjbJ	2.01	1.9E-04	0.69	Putative cytoplasmic protein
STM2925	nlpD	2.01	2.8E-05	2.71	Lipoprotein

(21). Based on this regulatory mechanism, *ptsI* mutation results in increased non-phosphorylated EIICB^{Glc}, sequestration of Mlc by non-phosphorylated EIICB^{Glc}, and, as a consequence, up-regulation of Mlc-repressed genes (22). Up-regulation of *ptsG* and the *manXYZ* operon in response to inactivation of *ptsI* has been observed previously (22, 23).

ulaABC necessary for the utilization of L-ascorbate encodes EII components of ascorbate-specific PTS, EIIC, EIIB, and EIIA (24). Normally, *ulaABC* forms an operon with three other genes (*ulaDEF*), which are required for the utilization of L-ascorbate (24, 25), whereas the *ulaABC* genes (STM2342, STM2343 and STM2344), whose expression was up-regulated in *ptsI* mutants, forms an operon with genes (STM2340 and STM2341) encoding transketolase (Table 4). Another *ula* operon, comprised of six genes (STM4383 to STM4388), seems to be the typical Ula operon necessary for L-ascorbate utilization, uptake, and phosphorylation. *S. Typhimurium* possesses two copies of

the *ula* operon, and many bacteria possess two or more UlaA paralogues, including *E. coli*, which has three (25). The expression of *ulaC* (STM2344), the first gene of the *ulaABC* operon, was found to be increased approximately three-fold in *mlc* mutants (Fig. 2). Although the fold increase of *ulaC*, (i.e., the *ulaABC* operon), was less than that of *ptsG* (Fig. 2), the up-regulation of *ulaC* by *mlc* mutation shows that it is possible that this operon is involved in glucose-related metabolism. Further research is necessary to study role of the STM2340-2344 operon.

Down-regulation of the *pdu* and *tdc* operons

During anaerobic growth, *S. Typhimurium* can use 1,2-propanediol as an energy source but not as a carbon source (26). In *ptsI* mutants, the expression of the propanediol utilization (*pdu*) genes was greatly reduced (Table 3). Of the 21 genes that comprise the *pdu* operon (27), 17 were down-regulated in *ptsI* mutants (Fig. 3). In particular, the

Table 3. List of the highly induced genes in *ptsI* mutants

Locus tag	Gene name	Ratio (ptsI/wt)	<i>p</i> -value	B-value	Description
STM2041	pduD	0.06	3.2E-10	13.74	Propanediol utilization: dehydratase, medium subunit
STM2039	pudB	0.07	1.4E-10	14.45	Propanediol utilization: polyhedral bodies
STM2044	pduH	0.08	6.1E-10	13.20	Propanediol utilization: diol dehydratase reactivation
STM2042	pduE	0.09	1.1E-09	12.68	Propanediol utilization: dehydratase, small subunit
STM2040	pduC	0.09	3.4E-07	7.23	Propanediol utilization: dehydratase, large subunit
STM3244	tdcB	0.12	2.6E-07	7.52	Threonine dehydratase, catabolic
STM3241	tdcE	0.13	9.1E-07	6.24	Pyruvate formate-lyase 4/ 2-ketobutyrate formate-lyase
STM2045	pduJ	0.13	2.9E-09	11.84	Propanediol utilization: polyhedral bodies
STM3240	tdcG	0.15	9.0E-08	8.56	L-serine deaminase
STM2046	pduK	0.15	7.5E-08	8.74	Propanediol utilization: polyhedral bodies
STM4540		0.16	3.0E-05	2.63	Putative glucosamine-fructose-6-phosphate aminotransferase
STM2867	hilC	0.17	3.0E-06	5.04	Bacterial regulatory helix-turn-helix proteins, araC family
STM2043	pduG	0.17	2.4E-05	2.85	Propanediol utilization: diol dehydratase reactivation
STM3242	tdcD	0.17	5.8E-05	1.95	Propionate kinase/acetate kinase II, anaerobic
STM3243	tdcC	0.18	9.2E-08	8.54	HAAAP family, L-threonine/ L-serine permease, anaerobically inducible
STM1175	flgC	0.18	6.0E-07	6.65	Flagellar biosynthesis, cell-proximal portion of basal-body rod
STM1962	fliT	0.19	2.6E-07	7.51	Flagellar biosynthesis; possible export chaperone for FliD
STM1955	fliZ	0.19	2.4E-06	5.24	Putative regulator of FliA
STM3339	nanA	0.19	1.8E-06	5.54	N-acetylneuraminate lyase (aldolase)
STM3106	ansB	0.20	2.4E-04	0.45	Periplasmic L-asparaginase II
STM2051	pduP	0.21	1.2E-07	8.24	Propanediol utilization: CoA-dependent propionaldehyde dehydrogenase
STM1961	fliS	0.23	1.1E-05	3.71	Flagellar biosynthesis; repressor of class 3a and 3b operons (RflA activity)
STM1959	fliC	0.23	1.4E-07	8.14	Flagellar biosynthesis; flagellin, filament structural protein
STM2433	err	0.23	3.3E-07	7.25	PTS family, glucose-specific IIA component
STM4124	oxyS	0.25	1.4E-07	8.13	Stable RNA induced by oxidative stress
STM1916	cheY	0.25	5.4E-07	6.76	Chemotaxis regulator, transmits chemoreceptor signals to flagellar motor components
STM2055	pduU	0.34	4.4E-05	2.24	Propanediol utilization: polyhedral bodies
STM2049	pduN	0.35	4.3E-07	7.01	Propanediol utilization: polyhedral bodies
STM1973	fliJ	0.36	5.6E-05	1.99	Flagellar fliJ protein
STM4315	rtsA	0.37	7.4E-06	4.09	Putative AraC-type DNA-binding domain-containing protein
STM2900	invH	0.39	1.1E-06	6.06	Invasion protein
STM1183	flgK	0.39	2.1E-06	5.39	Flagellar biosynthesis, hook-filament junction protein 1
STM4539		0.39	3.0E-05	2.63	Putative glucosamine-fructose-6-phosphate aminotransferase
STM4458	yjgF	0.39	5.5E-06	4.39	Putative translation initiation inhibitor
STM0701	speF	0.40	3.3E-06	4.91	Ornithine decarboxylase isozyme, inducible

Table 3. Continued

Locus tag	Gene name	Ratio (ptsI/wt)	p-value	B-value	Description
STM4538		0.40	1.8E-05	3.14	Putative PTS permease
STM1300		0.40	2.8E-06	5.09	Putative periplasmic protein
STM2063	phsC	0.40	4.2E-06	4.68	Hydrogen sulfide production: membrane anchoring protein
STM4106	katG	0.40	2.0E-05	3.08	Catalase; hydroperoxidase HPI(I)
STM2649	trxC	0.40	1.7E-05	3.21	Thioredoxin 2, redox factor
STM1971	fliH	0.41	2.5E-05	2.83	Flagellar biosynthesis; possible export of flagellar proteins
STM2865	avrA	0.41	1.2E-05	3.60	Putative inner membrane protein
STM3054	gcvH	0.42	9.6E-05	1.43	Glycine cleavage complex protein H, carrier of aminomethyl moiety via covalently bound lipoyl cofactor
STM4170	hupA	0.42	2.0E-04	0.66	DNA-binding protein HU-alpha (HU-2)
STM2893	invI	0.42	4.2E-05	2.30	Surface presentation of antigens; secretory proteins
STM1917	cheB	0.42	5.0E-06	4.50	Methyl esterase, response regulator for chemotaxis (cheA sensor)
STM1172	flgM	0.42	7.6E-06	4.06	Anti-FliA (anti-sigma) factor; also known as RflB protein
STM3156		0.43	6.9E-05	1.77	Putative cytoplasmic protein
STM0451	hupB	0.43	3.7E-05	2.41	DNA-binding protein HU-beta, NS1 (HU-1)
STM1301		0.43	1.8E-04	0.76	Putative mutator MutT protein
STM1976	fliM	0.43	9.0E-05	1.49	Flagellar biosynthesis, component of motor switch and energizing
STM4314	rtsB	0.44	1.4E-04	1.02	Putative bacterial regulatory proteins, luxR family
STM1838	yobF	0.44	4.9E-05	2.13	Putative cytoplasmic protein
STM4285	fdhF	0.44	7.6E-06	4.07	Formate dehydrogenase
STM2064	phsB	0.44	2.4E-05	2.89	Hydrogen sulfide production: iron- sulfur subunit; electron transfer
STM2056	pduV	0.34	1.5E-06	5.73	Propanediol utilization
STM2055	pduU	0.34	4.4E-05	2.24	Propanediol utilization: polyhedral bodies
STM2049	pduN	0.35	4.3E-07	7.01	Propanediol utilization: polyhedral bodies
STM1973	fliJ	0.36	5.6E-05	1.99	Flagellar fliJ protein
STM4315	rtsA	0.37	7.4E-06	4.09	Putative AraC-type DNA-binding domain-containing protein
STM2900	invH	0.39	1.1E-06	6.06	Invasion protein
STM1183	flgK	0.39	2.1E-06	5.39	Flagellar biosynthesis, hook-filament junction protein 1
STM4539		0.39	3.0E-05	2.63	Putative glucosamine-fructose-6-phosphate aminotransferase
STM4458	yjgF	0.39	5.5E-06	4.39	Putative translation initiation inhibitor
STM0701	speF	0.40	3.3E-06	4.91	Ornithine decarboxylase isozyme, inducible
STM4538		0.40	1.8E-05	3.14	Putative PTS permease
STM1300		0.40	2.8E-06	5.09	Putative periplasmic protein
STM2063	phsC	0.40	4.2E-06	4.68	Hydrogen sulfide production: membrane anchoring protein
STM4106	katG	0.40	2.0E-05	3.08	Catalase; hydroperoxidase HPI (I)
STM2649	trxC	0.40	1.7E-05	3.21	Thioredoxin 2, redox factor
STM1971	fliH	0.41	2.5E-05	2.83	Flagellar biosynthesis; possible export of flagellar proteins

Table 3. Continued

Locus tag	Gene name	Ratio (ptsI/wt)	p-value	B-value	Description
STM2865	avrA	0.41	1.2E-05	3.60	Putative inner membrane protein
STM3054	gcvH	0.42	9.6E-05	1.43	Glycine cleavage complex protein H, carrier of aminomethyl moiety via covalently bound lipoyl cofactor
STM4170	hupA	0.42	2.0E-04	0.66	DNA-binding protein HU-alpha (HU-2)
STM2893	invI	0.42	4.2E-05	2.30	Surface presentation of antigens; secretory proteins
STM1917	cheB	0.42	5.0E-06	4.50	Methyl esterase, response regulator for chemotaxis (cheA sensor)
STM1172	flgM	0.42	7.6E-06	4.06	Anti-FliA (anti-sigma) factor; also known as RflB protein
STM3156		0.43	6.9E-05	1.77	Putative cytoplasmic protein
STM0451	hupB	0.43	3.7E-05	2.41	DNA-binding protein HU-beta, NS1 (HU-1)
STM1301		0.43	1.8E-04	0.76	Putative mutator MutT protein
STM1976	fliM	0.43	9.0E-05	1.49	Flagellar biosynthesis, component of motor switch and energizing
STM4314	rtsB	0.44	1.4E-04	1.02	Putative bacterial regulatory proteins, luxR family
STM1838	yobF	0.44	4.9E-05	2.13	Putative cytoplasmic protein
STM4285	fdhF	0.44	7.6E-06	4.07	Formate dehydrogenase
STM2064	phsB	0.44	2.4E-05	2.89	Hydrogen sulfide production: iron- sulfur subunit; electron transfer
STM1969	fliF	0.45	1.1E-04	1.26	Flagellar biosynthesis; basal-body MS (membrane and supramembrane)-ring and collar protein
STM2877	iagB	0.45	4.1E-05	2.30	Cell invasion protein
STM1130		0.45	1.8E-04	0.78	Putative inner membrane protein
STM0871	ybjM	0.45	1.8E-05	3.15	Putative inner membrane protein
STM1924	flhC	0.46	2.0E-05	3.08	Regulator of flagellar biosynthesis, acts on class 2 operons
STM4340	firdD	0.46	2.5E-04	0.43	Fumarate reductase, anaerobic, membrane anchor polypeptide
STM4535		0.46	1.8E-04	0.79	Putative PTS permease
STM1171	flgN	0.47	2.5E-05	2.82	Flagellar biosynthesis: believed to be export chaperone for FlgK and FlgL
STM2876	hilA	0.47	2.6E-05	2.79	Invasion genes transcription activator
STM2153	yehE	0.48	1.3E-05	3.53	Putative outer membrane protein
STM0327		0.48	3.2E-05	2.56	Putative cytoplasmic protein
STM2868		0.48	1.4E-05	3.43	Putative cytoplasmic protein
STM1925	flhD	0.49	4.6E-05	2.18	Regulator of flagellar biosynthesis, acts on class 2 operons
STM3611	yhjH	0.49	2.7E-05	2.73	Putative Diguanylate cyclase/phosphodiesterase domain 3
STM1977	fliN	0.49	7.9E-05	1.62	Flagellar biosynthesis, component of motor switch and energizing
STM1182	flgJ	0.49	4.3E-05	2.25	Flagellar biosynthesis
STM2238		0.49	1.6E-04	0.86	Putative phage protein
STM2413	yfeC	0.49	3.5E-05	2.48	Putative negative regulator
STM3850	yieF	0.49	2.9E-04	0.26	Putative oxidoreductase
STM1918	cheR	0.49	1.8E-05	3.16	Glutamate methyltransferase, response regulator for chemotaxis
STM2414	yfeD	0.49	1.1E-04	1.31	Putative negative regulator

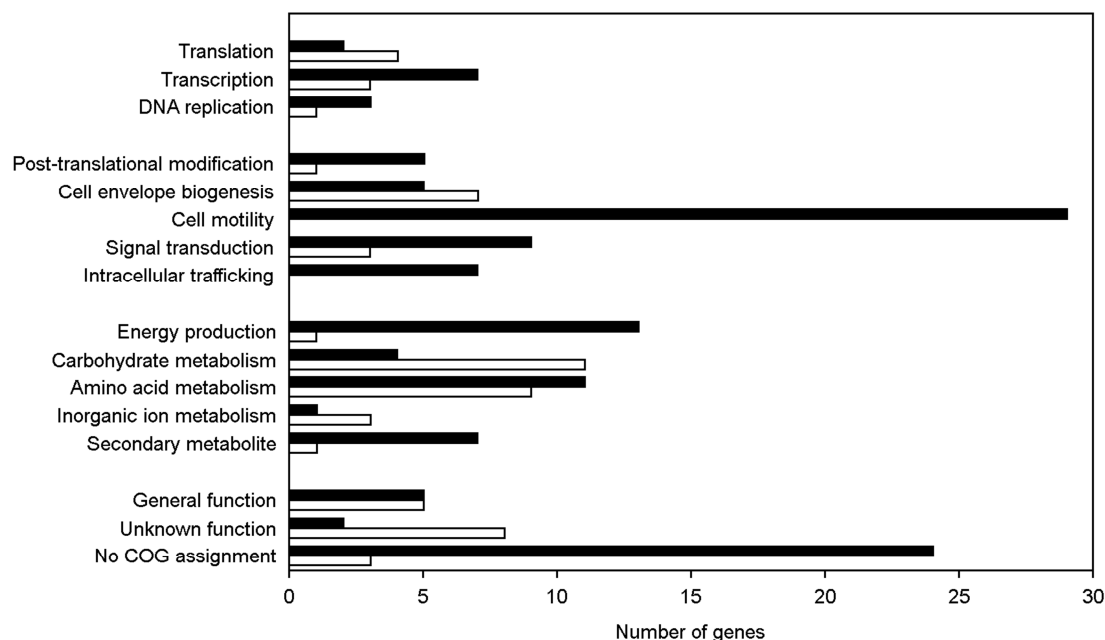


Figure 1. Distribution of differentially expressed genes. The genes whose expression was changed in the *ptsI* mutant were grouped into COG functional categories. The bars (black, down-regulated; and white, up-regulated) represent the number of genes in each COG category.

expression of *pduCDE* genes encoding propanediol dehydrogenase, which catalyze the first enzyme reaction in the propanediol fermentation pathway (26), was reduced more than 10-fold (Fig. 3). The *pdu* genes are *in vivo*-induced genes (28), and the Pdu proteins are present in macrophage-like culture conditions (29). In addition, *pdu* mutation impairs the intracellular replication of *S. Typhimurium* (30) and results in virulence defects in mice (28). Therefore, the reduced expression of *pdu* genes can contribute to the attenuation of the *ptsI* mutant strain. All the entire *tdc* operon genes, *tdcABCDEFG*, were down-regulated in *ptsI* mutants (Fig. 3). The Tdc proteins form an anaerobic pathway that degrades L-serine and L-threonine to acetate and propionate, respectively, and provide the cell with energy-rich keto acids that are catabolized to produce ATP via substrate-level phosphorylation (19). However, a mutation in *tdcA*, which encodes the transcriptional activator of the *tdc* operon, reduces the ability of *S. Typhimurium* to invade and to replicate within host cells, thereby causing attenuation (31, 32). Taken together, reduced expression of the *pdu* and

tdc operons, which are associated with energy acquisition and virulence, likely underlie, at least in part, the attenuation of the *ptsI* mutant strain.

Down-regulation of the flagellar genes

It is apparent that the majority of genes reduced by *ptsI* mutation under low-oxygen conditions are associated with cell motility (Fig. 1). Flagella biogenesis in *S. Typhimurium* involves more than 50 genes, which constitute at least 17 operons (33). Of these genes, 28, including the flagella synthesis operons (*flg* and *fli*), and the chemotaxis-associated genes, such as *cheY*, which encodes a chemotaxis signaling protein, were repressed in the *ptsI* mutant strain (Fig. 4). The reduced expression of the *flhDC*, *fliA*, *fliZ*, and *flgM* genes, which encode regulators of flagellar gene expression, and the *fliC* gene, which encodes the major flagella subunit, were confirmed by qRT-PCR (Fig. 5A). The qRT-PCR and microarray data were consistent in terms of overall changes in gene expression. Because the production of flagella increases under low-oxygen conditions (34), this result implies

that the negative effect of a *ptsI* mutation on the flagellar genes is most evident under optimal flagella expression

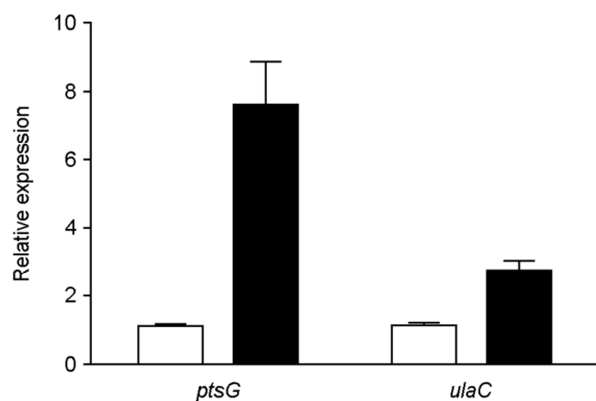


Figure 2. mRNA levels of *ulaC* (STM2344) in *mlc* mutants. Bacterial cultures were grown statically to mid-log phase. After total RNA isolation, qRT-PCR analysis was performed to determine *ptsG* and *ulaC* transcript levels. mRNA levels of each gene in the wild type were arbitrarily set to 1 (white bars), and then the relative expression of each *mlc* mutant gene (black bars) was determined by normalizing the mRNA levels to this value. Error bars indicate the standard deviations obtained in three independent experiments performed in duplicate.

conditions.

In many bacterial species, the flagellum is an acknowledged virulence factor, and non-flagellated strains been observed to be less virulent in several studies. Motility toward a host cell is a prerequisite for adhesion and invasion, and flagella can play an essential role in colonization by facilitating bacterial motility, even if the flagella do not directly participate in adhesion or invasion (35). A motility assay was performed using semi-solid agar plates (0.35% LB-agar) to examine the effect of *ptsI* on motility. The growth halo of *ptsI* mutants after 7 h of incubation was smaller (0.1 cm) than that of the wild-type strain (0.4 cm). After 14 h of incubation, *ptsI* mutants were clearly much less motile than wild type (Fig. 5B). Mutations in flagella genes have been noted to reduce virulence in *Salmonella* strains. *S. Typhimurium* strains carrying a null mutation in either of the flagella regulatory genes, *flhDC* or *fliA*, were less able to enter cultured epithelial cells (36). The *S. Typhimurium* mutant without flagella (*fliC/fliB* mutant) has significantly reduced invasion into epithelial cells and uptake into macrophage cells (37). The *cheB* mutant phenotype paralleled

Table 4. List of the highly induced genes in *ptsI* mutants

Locus tag	Gene	Description	Expression ratio
STM2342	<i>ulaA</i>	Ascorbate-specific PTS system EIIC	53.09
STM2341		Putative transketolase	46.19
STM2340		Putative transketolase	33.89
STM2344	<i>ulaC</i>	Putative PTS system EIIC component	26.92
STM3685	<i>mtlA</i>	Mannitol-specific EIIBC components	26.79
STM2343	<i>ulaB</i>	PTS system EIIB component	21.69
STM3686	<i>mtlD</i>	Mannitol-1-phosphate dehydrogenase	15.80
STM2339	<i>yfcC</i>	Putative integral membrane protein	12.87
STM3687	<i>mtlR</i>	Repressor for <i>mtl</i>	7.76
STM2458	<i>eutB</i>	Ethanolamine ammonia-lyase, heavy chain	6.00
STM2462	<i>eutJ</i>	Paral putative heatshock protein (Hsp70)	5.38
STM1203	<i>ptsG</i>	Glucose-specific EIIBC component	5.03
STM2456	<i>eutL</i>	Ethanolamine utilization	4.55
STM2459	<i>eutA</i>	Chaperonin in ethanolamine utilization	4.24

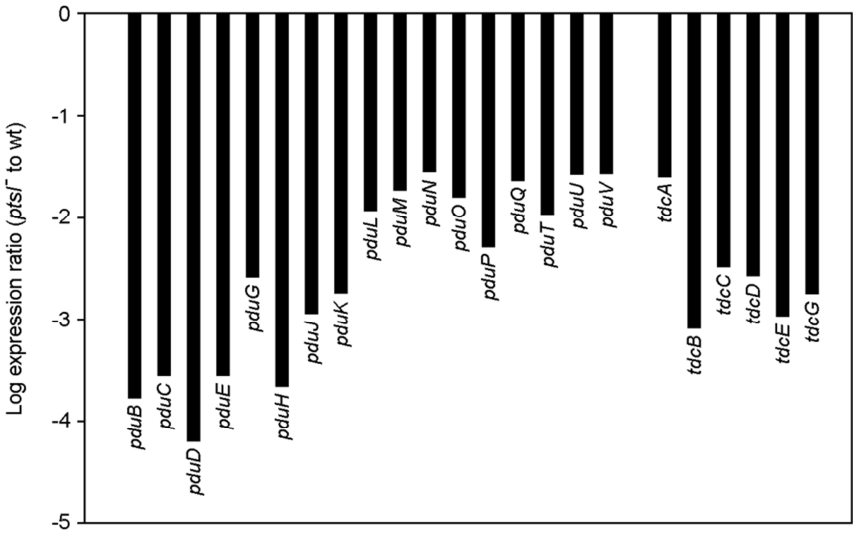


Figure 3. The fold change for the *pdu* and *tdc* genes. Bars represent the expression ratio (*ptsI* to wt) for each gene, which was derived from the \log_2 -transformed microarray hybridization results.

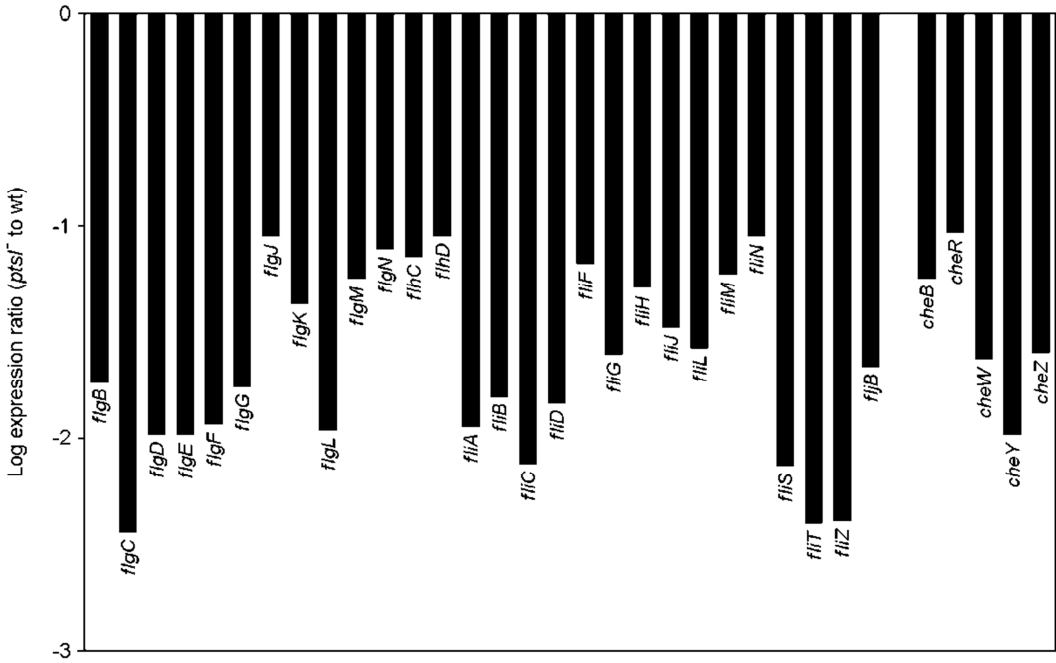


Figure 4. The fold change for the flagella and chemotaxis genes. Bars represent the expression ratio (*ptsI* to wt) for each gene, which was derived from the \log_2 -transformed microarray hybridization results.

that of the flagella-less *S. Typhimurium* mutant. The invasion ability of *ptsI* mutants was also examined, and a reduction in invasion for HEp-2 epithelial (approximately 40%) and RAW 264.7 macrophage (approximately 50%) cells was

observed (Fig. 5C). Therefore, the reduction in flagellar gene expression caused by the *ptsI* mutation is one of the reasons the *ptsI* mutant showed a reduction in invasion ability.

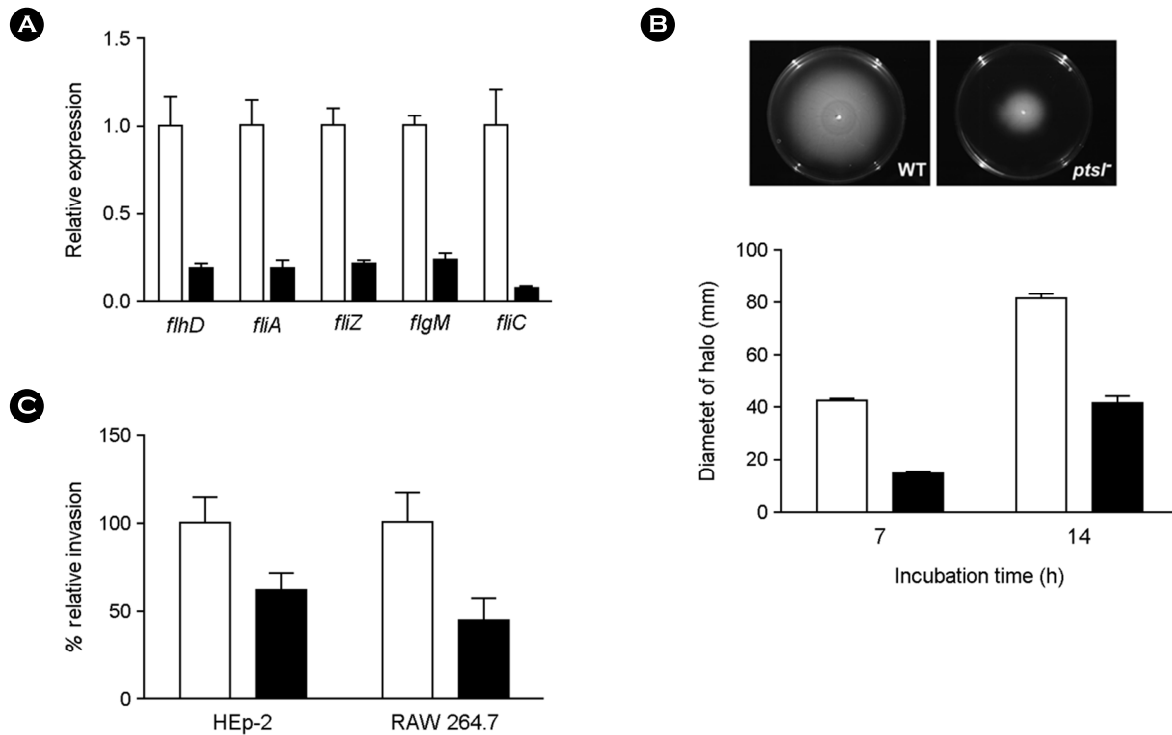


Figure 5. Defects in flagella biosynthesis in *ptsI* mutants. In all bar graphs, white and black bars represent the wild-type (WT) and *ptsI* mutant (*ptsI*⁻) mutant strains, respectively. (A) Validation of microarray results for five flagellar genes. mRNA levels were measured through qRT-PCR, and the mRNA levels of each gene in WT were set to 1. Error bars indicate the standard deviations (SD) obtained in three independent experiments performed in duplicate. (B) WT and *ptsI*⁻ were compared for motility. Bar graphs show the mean halo diameters (zones of motility) \pm SDs obtained from a quantitative motility assay performed in triplicate. The zone of motility was measured at 7 and 14 h after inoculation. (C) *Salmonella* invasion into HEp-2 epithelial and RAW 264.7 macrophage cells. The mammalian cells infected by WT and *ptsI*⁻ were lysed 2 h after infection and dilutions of the suspension were plated on LB agar medium to determine CFU. Data are presented as percentages of CFU of WT. Values are the means \pm SDs obtained in three independent experiments performed in duplicate.

DISCUSSION

Phosphoenolpyruvate (PEP) translocation, also known as the phosphotransferase system (PTS), is involved in transporting many sugars into bacteria, including glucose, mannose, fructose, and cellobiose. In the process of PTS transport in *Salmonella*, a histidine residue on enzyme I (EI) encoded by the *ptsI* gene was first phosphorylated and subsequently transfer the phosphate to downstream protein, HPr (15). Although previous studies have observed that disruption of *ptsI* gene was associated with attenuated virulence in mouse enteritis model, the exact mechanism underlying the reduction in virulence has not been clearly

understood (16).

Adenylate cyclase (CyaA) catalyzes the synthesis of cyclic AMP (cAMP) from ATP. cAMP plays a role in the regulation of the transcription of many genes through binding to the cAMP receptor protein (CRP) (38). Because the phosphorylated form of EIIA^{Glc} stimulates CyaA activity, cAMP levels are low in mutants that are unable to form phosphorylated EIIA^{Glc} (4). The expression of flagellar genes is coordinately regulated by *flhDC*, which is a major regulator of all genes in the flagellar cascade (33). *flhDC* expression is influenced at the transcriptional level by cAMP-CRP binding (39). Considering the underlying mechanism for the enhanced expression of *ptsG* in *ptsI* mutants (21), it is likely that the *ptsI* mutation results in non-

phosphorylated EIIA^{Glc}, thereby reducing CyaA activity. This suggests that a defect in flagella biosynthesis is correlated with the low cAMP level in *ptsI* mutants. It should also be noted that the cAMP-CRP complex is necessary for the expression of the *pdu* and *tdc* operons (21).

The present study used microarray analysis to determine why *ptsI* mutant virulence, motility, and invasion are attenuated. The expression of *pdu*, *tdc*, and flagella genes, which encode proteins involved in *Salmonella* virulence, was greatly reduced in *ptsI* mutants (Table 3). However, these genes share characteristics in terms of oxygen level: (i) the Pdu and Tdc proteins are associated with energy acquisition under low-oxygen conditions (19, 40) and (ii) the production of Tdc and flagella increases in response to the low oxygen level (19, 34). Thus, more studies that examine the alteration of gene expression in *ptsI* mutants under different environmental conditions are needed to fully delineate the mechanisms of its attenuation.

REFERENCES

- 1) Coburn B, Grassl GA, Finlay BB. *Salmonella*, the host and disease: a brief review. *Immunol Cell Biol* 2007; 85:112-8.
- 2) Finlay BB, Brumell JH. *Salmonella* interactions with host cells: *in vitro* to *in vivo*. *Philos Trans R Soc Lond B Biol Sci* 2000;355:623-31.
- 3) Ohl ME, Miller SI. *Salmonella*: a model for bacterial pathogenesis. *Annu Rev Med* 2001;52:259-74.
- 4) Görke B, Stülke J. Carbon catabolite repression in bacteria: many ways to make the most out of nutrients. *Nat Rev Microbiol* 2008;6:613-24.
- 5) Eisenreich W, Dandekar T, Heesemann J, Goebel W. Carbon metabolism of intracellular bacterial pathogens and possible links to virulence. *Nat Rev Microbiol* 2010; 8:401-12.
- 6) Clements M, Eriksson S, Tezcan-Merdol D, Hinton JC, Rhen M. Virulence gene regulation in *Salmonella enterica*. *Ann Med* 2001;33:178-85.
- 7) Rhen M, Dorman CJ. Hierarchical gene regulators adapt *Salmonella enterica* to its host milieu. *Int J Med Microbiol* 2005;294:487-502.
- 8) Poncet S, Milohanic E, Mazé A, Nait Abdallah J, Aké F, Larribe M, *et al.* Correlations between carbon metabolism and virulence in bacteria. *Contrib Microbiol* 2009;16:88-102.
- 9) Le Bouguénec C, Schouler C. Sugar metabolism, an additional virulence factor in enterobacteria. *Int J Med Microbiol* 2011;301:1-6.
- 10) Hautefort I, Thompson A, Eriksson-Ygberg S, Parker ML, Lucchini S, Danino V, *et al.* During infection of epithelial cells *Salmonella enterica* serovar Typhimurium undergoes a time-dependent transcriptional adaptation that results in simultaneous expression of three type 3 secretion systems. *Cell Microbiol* 2008;10:958-84.
- 11) Götz A, Eylert E, Eisenreich W, Goebel W. Carbon metabolism of enterobacterial human pathogens growing in epithelial colorectal adenocarcinoma (Caco-2) cells. *PloS One* 2010;5:e10586.
- 12) Eriksson S, Lucchini S, Thompson A, Rhen M, Hinton JC. Unravelling the biology of macrophage infection by gene expression profiling of intracellular *Salmonella enterica*. *Mol Microbiol* 2003;47:103-18.
- 13) Bowden SD, Hopper-Chidlaw AC, Rice CJ, Ramachandran VK, Kelly DJ, Thompson A. Nutritional and metabolic requirements for the infection of HeLa cells by *Salmonella enterica* serovar Typhimurium. *PloS One* 2014;9: e96266.
- 14) Bowden SD, Rowley G, Hinton JC, Thompson A. Glucose and glycolysis are required for the successful infection of macrophages and mice by *Salmonella enterica* serovar typhimurium. *Infect Immun* 2009;77:3117-26.
- 15) Deutscher J, Francke C, Postma PW. How phosphotransferase system-related protein phosphorylation regulates carbohydrate metabolism in bacteria. *Microbiol Mol Biol Rev* 2006;70:939-1031.
- 16) Kok M, Bron G, Erni B, Mukhija S. Effect of enzyme I of the bacterial phosphoenolpyruvate: sugar phosphotransferase system (PTS) on virulence in a murine model. *Microbiology* 2003;149:2645-52.
- 17) Shin D, Cho N, Kim YJ, Seok YJ, Ryu S. Up-regulation of the cellular level of *Escherichia coli* PTS components by stabilizing reduced transcripts of the genes in response to the low oxygen level. *Biochem Biophys Res Commun* 2008;370:609-12.
- 18) Lim S, Yun J, Yoon H, Park C, Kim B, Jeon B, *et al.* Mlc regulation of *Salmonella* pathogenicity island I gene expression via hIle repression. *Nucleic Acids Res*

- 2007;35:1822-32.
- 19) Kim MJ, Lim S, Ryu S. Molecular analysis of the *Salmonella* typhimurium *tdc* operon regulation. J Microbiol Biotechnol 2008;18:1024-32.
- 20) Lonnstedt I ST. Replicated microarray data. Statistica Sinica 2002;12:31-46.
- 21) Plumbridge J. Regulation of gene expression in the PTS in *Escherichia coli*: the role and interactions of Mlc. Curr Opin Microbiol 2002;5:187-93.
- 22) Plumbridge J. A mutation which affects both the specificity of PtsG sugar transport and the regulation of *ptsG* expression by Mlc in *Escherichia coli*. Microbiology 2000;146:2655-63.
- 23) Zeppenfeld T, Larisch C, Lengeler JW, Jahreis K. Glucose transporter mutants of *Escherichia coli* K-12 with changes in substrate recognition of IICB (Glc) and induction behavior of the *ptsG* gene. J Bacteriol 2000;182:4443-52.
- 24) Yew WS, Gerlt JA. Utilization of L-ascorbate by *Escherichia coli* K-12: assignments of functions to products of the *yjf-sga* and *yia-sgb* operons. J Bacteriol 2002;184:302-6.
- 25) Zhang Z, Aboulwafa M, Smith MH, Saier MH Jr. The ascorbate transporter of *Escherichia coli*. J Bacteriol 2003;185:2243-50.
- 26) Bobik TA, Xu Y, Jeter RM, Otto KE, Roth JR. Propanediol utilization genes (*pdu*) of *Salmonella* typhimurium: three genes for the propanediol dehydratase. J Bacteriol 1997;179:6633-9.
- 27) Bobik TA, Havemann GD, Busch RJ, Williams DS, Aldrich HC. The propanediol utilization (*pdu*) operon of *Salmonella enterica* serovar Typhimurium LT2 includes genes necessary for formation of polyhedral organelles involved in coenzyme B(12)-dependent 1, 2-propanediol degradation. J Bacteriol 1999;181:5967-75.
- 28) Conner CP, Heithoff DM, Julio SM, Sinsheimer RL, Mahan MJ. Differential patterns of acquired virulence genes distinguish *Salmonella* strains. Proc Natl Acad Sci U S A 1998;95:4641-5.
- 29) Adkins JN, Mottaz HM, Norbeck AD, Gustin JK, Rue J, Clauss TR, et al. Analysis of the *Salmonella* typhimurium proteome through environmental response toward infectious conditions. Mol Cell Proteomics 2006;5:1450-61.
- 30) Klumpp J, Fuchs TM. Identification of novel genes in genomic islands that contribute to *Salmonella* typhimurium replication in macrophages. Microbiology 2007;153:1207-20.
- 31) Kim M, Lim S, Kim D, Choy HE, Ryu S. A *tdcA* mutation reduces the invasive ability of *Salmonella enterica* serovar typhimurium. Mol Cells 2009;28:389-95.
- 32) Lim S, Kim M, Choi J, Ryu S. A mutation in *tdcA* attenuates the virulence of *Salmonella enterica* serovar Typhimurium. Mol Cells 2010;29:509-17.
- 33) Soutourina OA, Bertin PN. Regulation cascade of flagellar expression in Gram-negative bacteria. FEMS microbiol Rev 2003;27:505-23.
- 34) Landini P, Zehnder AJ. The global regulatory *hns* gene negatively affects adhesion to solid surfaces by anaerobically grown *Escherichia coli* by modulating expression of flagellar genes and lipopolysaccharide production. J Bacteriol 2002;184:1522-9.
- 35) Haiko J, Westerlund-Wikstrom B. The role of the bacterial flagellum in adhesion and virulence. Biology 2013;2:1242-67.
- 36) Eichelberg K, Galán JE. The flagellar sigma factor FliA (sigma(28)) regulates the expression of *Salmonella* genes associated with the centisome 63 type III secretion system. Infect Immun 2000;68:2735-43.
- 37) Olsen JE, Hoegh-Andersen KH, Casadesús J, Rosenkranz J, Chadfield MS, Thomsen LE. The role of flagella and chemotaxis genes in host pathogen interaction of the host adapted *Salmonella enterica* serovar Dublin compared to the broad host range serovar *S. Typhimurium*. BMC microbiol 2013;13:67.
- 38) Postma PW, Lengeler JW, Jacobson GR. Phosphoenolpyruvate:carbohydrate phosphotransferase systems of bacteria. Microbiol Rev 1993;57:543-94.
- 39) Chilcott GS, Hughes KT. Coupling of flagellar gene expression to flagellar assembly in *Salmonella enterica* serovar typhimurium and *Escherichia coli*. Microbiol Mol Biol Rev 2000;64:694-708.
- 40) Hesslinger C, Fairhurst SA, Sawers G. Novel keto acid formate-lyase and propionate kinase enzymes are components of an anaerobic pathway in *Escherichia coli* that degrades L-threonine to propionate. Mol Microbiol 1998;27:477-92.